Molecular Biology of the Cell
Vol. 18, 4837–4846, December 2007

p21$^{waf1/cip1/sdi1}$ as a Central Regulator of Inducible Smooth Muscle Actin Expression and Differentiation of Cardiac Fibroblasts to Myofibroblasts

Sashwati Roy,* Savita Khanna,* Trenton Rink,* Jared Radtke,* W. Taylor Williams,* Sabyasachi Biswas,* Rebecca Schnitt,* Arthur R. Strauch,† and Chandan K. Sen*

*Laboratory of Molecular Medicine, Department of Surgery, and †Department of Physiology and Cell Biology, Davis Heart and Lung Research Institute, The Ohio State University Medical Center, Columbus, OH 43210

Submitted March 23, 2007; Revised August 1, 2007; Accepted September 11, 2007
Monitoring Editor: Carl-Henrik Heldin

The phenotypic switch of cardiac fibroblasts (CFs) to myofibroblasts is essential for normal and pathological wound healing. Relative hyperoxic challenge during reoxygenation causes myocardial remodeling. Here, we sought to characterize the novel O_2-sensitive molecular mechanisms responsible for triggering the differentiation of CFs to myofibroblasts. Exposure of CFs to hyperoxic challenge–induced transcription of smooth muscle actin (SMA) and enhanced the stability of both Acta2 transcript as well as of SMA protein. Both p21 deficiency as well as knockdown blunted hyperoxia-induced Acta2 and SMA response. Strikingly, overexpression of p21 alone markedly induced differentiation of CFs under normoxia. Overexpression of p21 alone induced SMA transcription by down-regulating YB1 and independent of TGFβ1. In vivo, hyperoxic challenge induced p21-dependent differentiation of CFs to myofibroblasts in the infarct boundary region of ischemia-reperfused heart. Tissue elements were laser-captured from infarct boundary and from a noninfarct region 0.5 mm away. Reperfusion caused marked p21 induction in the infarct region. Acta2 as well as SMA expression were markedly up-regulated in CF-rich infarct boundary region. Of note, ischemia-reperfusion–induced up-regulation of Acta2 in the infarct region was completely abrogated in p21-deficient mice. This observation establishes p21 as a central regulator of reperfusion-induced phenotypic switch of CFs to myofibroblasts.

INTRODUCTION

Cardiac fibroblasts (CFs) represent the most abundant cell type in the heart constituting two-thirds of the total cell population in the myocardium. CFs regulate cardiomyocyte biology as well as myocardial angiogenesis (Sen *et al.*, 2006; Laframboise *et al.*, 2007). The phenotypic switch of CFs to myofibroblasts, with acquisition of specialized contractile features, is essential for connective-tissue remodeling during normal and pathological wound healing (Frangogiannis, 2006). Cardiac myofibroblasts are specialized contractile fibroblasts formed by irreversible acquisition of contractile proteins such as smooth muscle actin (SMA). In normal wound healing, differentiation to myofibroblasts is necessary for repair and stabilization, but these cells eventually undergo apoptosis. If myofibroblasts remain in the injured area for an extended period of time, excessive extracellular matrix (ECM) production occurs, resulting in fibrosis that in turn leads to loss of myocardial compliance (Weber and Brilla, 1991; Brilla, 2000; Burlew and Weber, 2002). Such a condition is commonly noted in patients who have suffered from myocardial infarction and those suffering from heart failure and often leads to further loss of cardiac function (Capasso *et al.*, 1990; Sun *et al.*, 2000). Regardless of etiology, cardiac fibrosis is a major contributor to cardiac remodeling associated with cardiomyopathies. It is characterized by expansion of the interstitial compartment due to increased deposition of extracellular matrix by activated myofibroblasts. Apart from their role in structural remodeling, myofibroblasts might contribute to arrhythmogenesis by direct modulation of myocardial conduction (Miragoli *et al.*, 2006). The phenotypic switch of CFs to myofibroblasts is therefore of key clinical significance, and the mechanisms underlying such transformation has been of critical interest (Cucoranu *et al.*, 2005; Swaney *et al.*, 2005; Naugle *et al.*, 2006).

We have recently demonstrated that reoxygenation of a focal ischemic site of the heart, in addition to being a trigger for reperfusion injury, induces tissue remodeling (Roy *et al.*, 2003a,b; Sen *et al.*, 2006). Focal ischemia in the heart results in a hypoxic area containing a central focus of near-zero O_2 pressure bordered by tissue with diminished but nonzero O_2 pressures. These border zones extend for several millimeters from the hypoxic core, with the O_2 pressures progressively increasing from the focus to the normoxic region (Sen *et al.*, 2006). Moderate hypoxia is associated with a 30–60% decrease (~1–3%O_2) in pO_2 (Siaghy *et al.*, 2000). During chronic hypoxia in the heart, cells lower their normoxic set-point (Khanna *et al.*, 2006) such that the return to normoxic pO_2 after chronic hypoxia results in perceived hyperoxia (Roy *et al.*, 2003a,b, 2006a; Kuhn *et al.*, 2006, 2007; Sen *et al.*, 2006). Compared with myocytes, CFs are relatively more resistant to oxygen toxicity (Zhang *et al.*, 2001; Liao *et al.*, 2004). As a result, the infarct site, devoid of myocytes, continues to be populated by CFs (Kuhn *et al.*, 2006, 2007). Perceived hyper-

This article was published online ahead of print in *MBC in Press* (http://www.molbiolcell.org/cgi/doi/10.1091/mbc.E07–03–0270) on September 19, 2007.

Address correspondence to: Chandan K. Sen (chandan.sen@osumc.edu).

oxia induces differentiation of CFs to myofibroblasts at the infarct site (Sen *et al.*, 2006). We have previously noted that CFs, isolated from adult murine ventricle, cultured in 10 or 20% O_2 (high O_2, *relative* to the pO_2 to which cells are adjusted in vivo), compared with 3% O_2 (mildly hypoxic), exhibit reversible growth inhibition and a phenotypic switch indicative of differentiation (Roy *et al.*, 2003a). These observations led to the hypothesis that marginal relative elevation in pO_2, compared with pO_2 to which cells are adjusted during chronic moderate hypoxia, serve as a signal to trigger CF differentiation. In this study, we sought to characterize the novel O_2-sensitive molecular mechanisms responsible for triggering the differentiation of CFs to myofibroblasts. This work provides first evidence demonstrating that the cell cycle inhibitor $p21^{waf1/cip1/sdi1}$, the significance of which in the heart is poorly understood, is sufficient to induce a phenotypic switch of CFs to myofibroblasts. This novel observation is likely to be highly significant to understand fibrosis across various organs.

MATERIALS AND METHODS

Cardiac Fibroblast Isolation and Culture

Experiments were performed using primary CFs isolated from adult (5–6 wk old) mouse ventricle using procedures described previously (Roy *et al.*, 2003a,b).

mRNA Quantitation

mRNA was quantified by real-time PCR assay using double-stranded DNA-binding dye SYBR green-I, as described previously (Roy *et al.*, 2003a,b, 2006a,b). The primer sets used for individual genes were as follows: mCDKN1A (p21) F: 5′ ACAGGAGCAAAGTGTGCCGTTGT 3′; mCDKN1A (p21) R: 5′ GCTCAGACACCAGAGTGCAAGACA 3′; mGAPDH F: 5′ ATGACCACAGTCCATGCCATCACT 3′; mGAPDH R: 5′ TGTTGAAGTCGCAGGAGACAACCT 3′; mActa2 F: 5′ GGCACCACTGAACCCTAAGG 3′; and mActa2 R: 5′ TCTCCAGAGTCCAGCACAAT 3′.

Immunofluorescence Microscopy

F-actin (phalloidin, dilution 1:40, Molecular Probes), α-smooth muscle actin (SMA, Sigma) and $p21^{Cip1/WAF1/Sdi1}$ (hereafter p21; Santa Cruz) immunostaining and microscopy (Zeiss Axiovert 200M) were performed as described (Roy *et al.*, 2003a,b; Roy *et al.*, 2003b).

Western Blot

Western blot was performed as described previously (Roy *et al.*, 2003a,b). Primary antibodies against SMA (1:4000, Sigma, St. Louis, MO), β-actin (1:5000 Sigma), and p21 (1:200 dilution) were used to detect the corresponding antigens.

CAT and EGFP Reporter Assays

The mouse SMA-CAT promoter-reporter construct used in this study has been described previously (Foster *et al.*, 1992). pVSMP8-EGFP was developed in our laboratories by Dr. Arthur Strauch. The VSMP8 promoter moiety consists of the 5′-flanking and first intronic regions of the mouse SMA gene (Min *et al.*, 1990). Commercial immunoassays were used to measure chloramphenicol acetyltransferase (CAT) reporter proteins as directed by the manufacturer (Promega, Madison, WI).

Cell Counting

Cells were seeded at 5000 cells/well in four-well plates. Before counting, cells were trypsinized and resuspended in a single cell suspension. Counting was performed using a Z1 series Coulter counter as described (Roy *et al.*, 2003a).

Cell Cycle Analysis

Cell cycle profiles were determined using a flow cytometer (Krishan, 1975) and CellQuest software (BD Biosciences, San Jose, CA).

Small Interference RNA Delivery

Lipofectamine 2000 reagent (Invitrogen Corporation, Carlsbad, CA) was used to transfect cells with 100 nM small interference RNA (siRNA) pool (Dharmacon RNA Technologies, Lafayette, CO) for 48 h as described (Khanna *et al.*, 2006). For control, siControl nontargeting siRNA pool (mixture of four siRNA, designed to have ≥4 mismatches with known mouse genes) was used.

Survival Model for Coronary Artery Occlusion and Reperfusion

C57BL/6, $p21^{-/-}$ and corresponding wild-type mice were subjected to ischemia-reperfusion of the heart as described previously (Roy *et al.*, 2003b, 2006a; Kuhn *et al.*, 2006). The studies were approved by the Institutional Laboratory Animal Care and Use Committee of The Ohio State University. Mice were anesthetized, intubated, and mechanically ventilated on a positive pressure respirator with room air. The body temperature was maintained at 36–37°C with a heated small-animal operating table. Left thoracotomy was performed via the fifth intercostal space to expose the heart. A 30-min occlusion of left anterior descending coronary artery (LAD) was followed by reperfusion. Laser Doppler flow measurement was used to verify ischemia and reperfusion. On successful reperfusion, the thorax was closed and negative thoracic pressure was reestablished for survival. The mice were killed 7 d after reperfusion. Hearts were either collected frozen in OCT compound for laser capture or in Formalin for histological analyses.

Laser Microdissection and Pressure Catapulting

Laser microdissection and pressure catapulting (LMPC) was performed using the Microlaser System from PALM Microlaser Technologies AG (Bernreid, Germany) as described (Kuhn *et al.*, 2006; Roy *et al.*, 2006a). Briefly, murine hearts with experimental ischemia-reperfusion were isolated, frozen in OCT compound, and then cut into 10-μm sections using a cryo-microtome. The sections were placed on PEN (polyethylene napthalate) membrane glass slides (PALM Microlaser Technologies AG) that had been RNAsin- (Ambion, Austin, TX) and UV-treated, for cutting and catapulting as described by our group recently (Kuhn *et al.*, 2006, 2007). Sections were stained using a modified hematoxylin QS procedure (Kuhn *et al.*, 2006, 2007), and the infarct site was identified as reported. Matched area of myocyte$^+$ control (*C*) and infarct (*I*) area were captured in chaotropic RNA lysis solution followed by mRNA quantitation as described (Kuhn *et al.*, 2006; Roy *et al.*, 2006a). RNA extraction, reverse transcription and mRNA quantitation using real-time PCR were performed as described (Kuhn *et al.*, 2006; Roy *et al.*, 2006a).

Histochemistry

Formalin-fixed tissues were embedded in paraffin and sectioned (4 μm) followed by Masson Trichrome staining. This procedure results in blue-black nuclei and blue collagen and cytoplasm. Muscle fibers stained red.

Statistics

In vitro data are reported as mean ± SD of at least three experiments. Comparisons among multiple groups were made by analysis of variance ANOVA. $p < 0.05$ was considered statistically significant. For in vivo studies data are reported as mean ± SEM of at least three experiments. Data from infarct (*I*) and corresponding control (*C*) regions of the same heart were tested on a paired basis. Comparisons among multiple groups were made by analysis of variance ANOVA. $p < 0.05$ was considered statistically significant.

RESULTS

Previously we have estimated that under resting conditions for mice breathing room air, the heart ventricular pO_2 is roughly 5% (Roy *et al.*, 2003a). Furthermore, we have established that comparison of results from CFs cultured at 5% O_2 (in vivo normoxia) with those cultured under standard conditions of 20% O_2 (hyperoxia) ambience represents an useful approach to study O_2-sensitive changes in the CFs relevant to perceived hyperoxia (Roy *et al.*, 2003a,b). In this study, we utilize the same approach. O_2-sensitive mechanisms, relevant to perceived hyperoxia in vivo (Roy *et al.*, 2003b, 2006a; Kuhn *et al.*, 2006, 2007; Sen *et al.*, 2006), were investigated by comparing results obtained from CFs cultured at 5% O_2 compared with matched cells of the same isolation cultured at 20% O_2. Next, the in vivo relevance of the in vitro findings were tested in a standardized model of ischemia-reperfusion (Roy *et al.*, 2003b, 2006a; Kuhn *et al.*, 2006, 2007). Irreversible acquisition of contractile proteins such as SMA represents a hallmark of the differentiation of CFs to myofibroblasts. Using CFs isolated from adult murine ventricles, we noted that exposure to hyperoxia potently induced Acta2, the gene that encodes SMA (Figure 1A). O_2-induced expression of Acta2 was associated with elevated expression of the corresponding protein, SMA (Figure 1B). To test whether the induction of Acta2 by elevated O_2 was transcriptionally

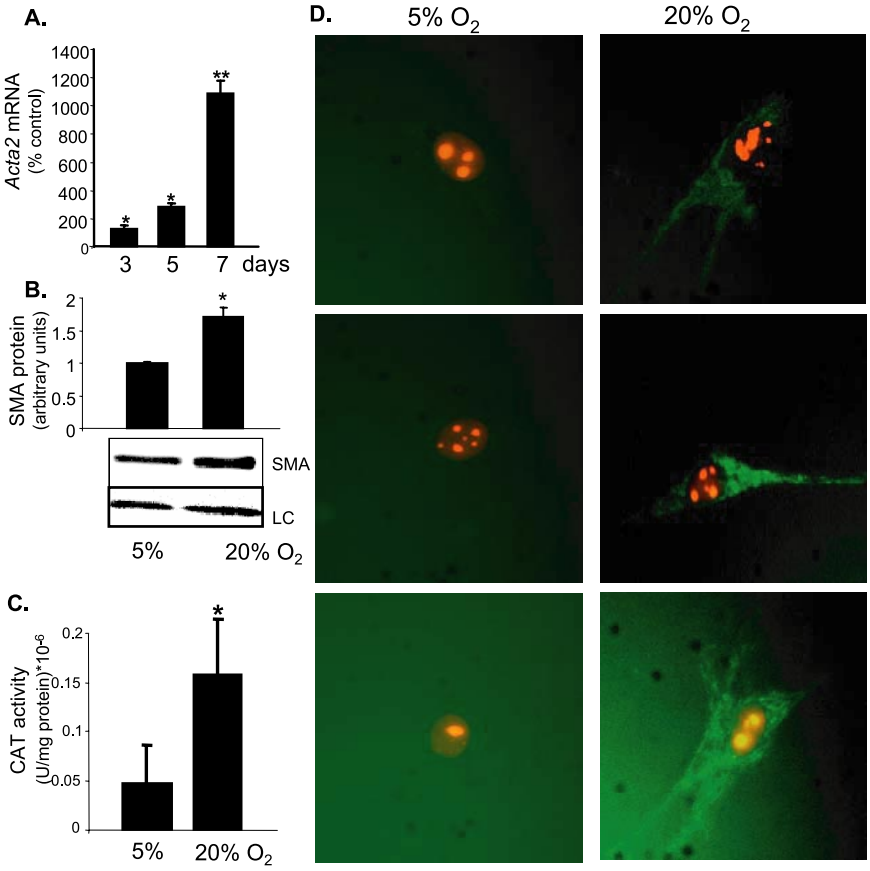

Figure 1. Oxygen-induced Acta2 expression. CFs isolated from C57BL/6 mouse (5–6 wk, male) heart ventricle were seeded at 5% (normoxia) or 20% (hyperoxia) O_2 and cultured for 5 d. After splitting, cells were either maintained in 5 or 20% O_2 ambience for the indicated periods of time. (A) Change in Acta2 mRNA levels in CFs at 20% O_2 compared with gene expression in cells gown at 5% O_2. Acta2 mRNA levels were determined using real-time PCR and normalized against GAPDH expression detected in the same samples. Data shown represent % change compared with control CFs grown at 5% O_2; mean ± SD; n = 4. *$p < 0.05$; significantly higher compared with data from cells in 5% O_2, **$p < 0.01$; significantly higher compared with cells in 5% O_2. (B) Western blot of α-smooth muscle actin (SMA) protein. Bar graph shown is the quantitative assessment of SMA protein levels on day 3 of exposure. Data were normalized to the protein loaded as detected by Ponceau staining of the membrane. LC, loading control. Data shown are mean ± SD; n = 3. (D) *$p < 0.05$; significantly higher compared with cells in 5% O_2. (C and D) After isolation, CFs were cultured at 5% O_2 for 5 d. After transfection of CFs with pVSMP reporter constructs, cells were further cultured at 5% O_2 for 18 h. Next, cells were transferred to 20% O_2 or retained in 5% O_2 as indicated in the illustration. SMA promoter activity was measured after 5 d. (C) To quantify Acta2 promoter activity, cells were transfected with pVSMP-CAT plasmid. CAT activity was determined from cell lysates as an indicator of SMA promoter activity. Result of reporter activities were normalized for the amount of the protein in cell lysates. Data are mean ± SD; n = 4. *$p < 0.05$; significantly higher compared with cells in 5% O_2. (D) CFs transfected with pVSMP-GFP reporter construct. To detect transfected cells, CFs were cotransfected with pDsRed2-Nuc (red, containing DsRed2 gene with nuclear localization signal). Activated (20% O_2) cells show nucleus (red) and green (GFP) fluorescence. Resting (5% O_2) cells show red nucleus only. Representative transfected cells under 5% O_2 or 20% O_2 are shown.

regulated, vascular smooth muscle promoter (VSMP)-reporter constructs were utilized. Clearly, hyperoxic exposure induced both VSMP-green fluorescent protein (GFP; Figure 1D) as well as VSMP-CAT (Figure 1C) reporters. These findings indicate that the transcription of SMA is sensitive to hyperoxic exposure. Next, we sought to examine whether hyperoxic challenge influenced Acta2 and its protein product. The stability of Acta2 mRNA and corresponding SMA protein were studied in cells treated with actinomycin D or cyclohexamide, respectively. Under conditions of hyperoxia Acta2 mRNA was significantly more stable than Acta2 mRNA in CFs grown at 5% O_2 (Figure 2A). Consistently, exposure to hyperoxia slowed the degradation of SMA resulting in higher levels of SMA in hyperoxia-challenged CFs (Figures 2, B and C).

Elevated O_2 caused an initial increase in SMA mRNA followed by a comparable rate of mRNA degradation in 5% O_2 and 20% O_2. The early response noted may represent a transcriptional induction of the ActaA2 gene by hyperoxia. Taken together, the findings reported above demonstrated that SMA expression in CFs is sensitive to hyperoxia at three levels of control: 1) transcription; 2) posttranscriptional stabilization of Acta2 mRNA; and 3) posttranscriptional stabilization of SMA protein.

Our previous work had identified that p21 deficiency abrogates hyperoxia-induced growth arrest of CFs (Roy *et al.*, 2003a). p21 being a well-characterized cell cycle inhibitor, the observation was not unexpected. The observation, however, did kindle our interest to question the functional sig-

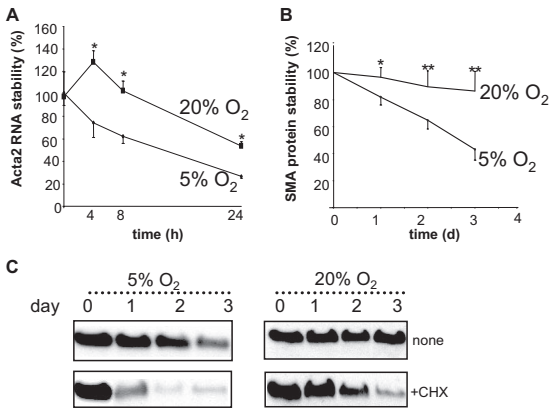

Figure 2. Oxygen-sensitive stabilization of Acta2 mRNA and SMA protein. After isolation, CFs were cultured at 5% O_2 for 5 d. Next, cells were transferred to 20% O_2 or retained in 5% O_2 and maintained in the respective O_2 ambience for 5 d. Cells were harvested for the determination of mRNA and protein stability at the time points specified. (A) Actinomycin D (5 μg/ml) was added to the cultures, and Acta2 mRNA levels were determined using real-time PCR. Data are mean ± SD; n = 4. (B) Cells were treated with cyclohexamide (20 μg/ml; CHX), and SMA protein levels were determined using Western blot and densitometry. (C) Densitometric data of blot shown in B. Stability of SMA in CFs gown in 5 or 20% O_2. SMA levels in presence of CHX were normalized to levels of SMA without CHX. Data shown are mean ± SD; n = 3. *$p < 0.05$; significantly higher compared with cells in 5% O_2, **$p < 0.01$; significantly higher compared with cells in 5% O_2.

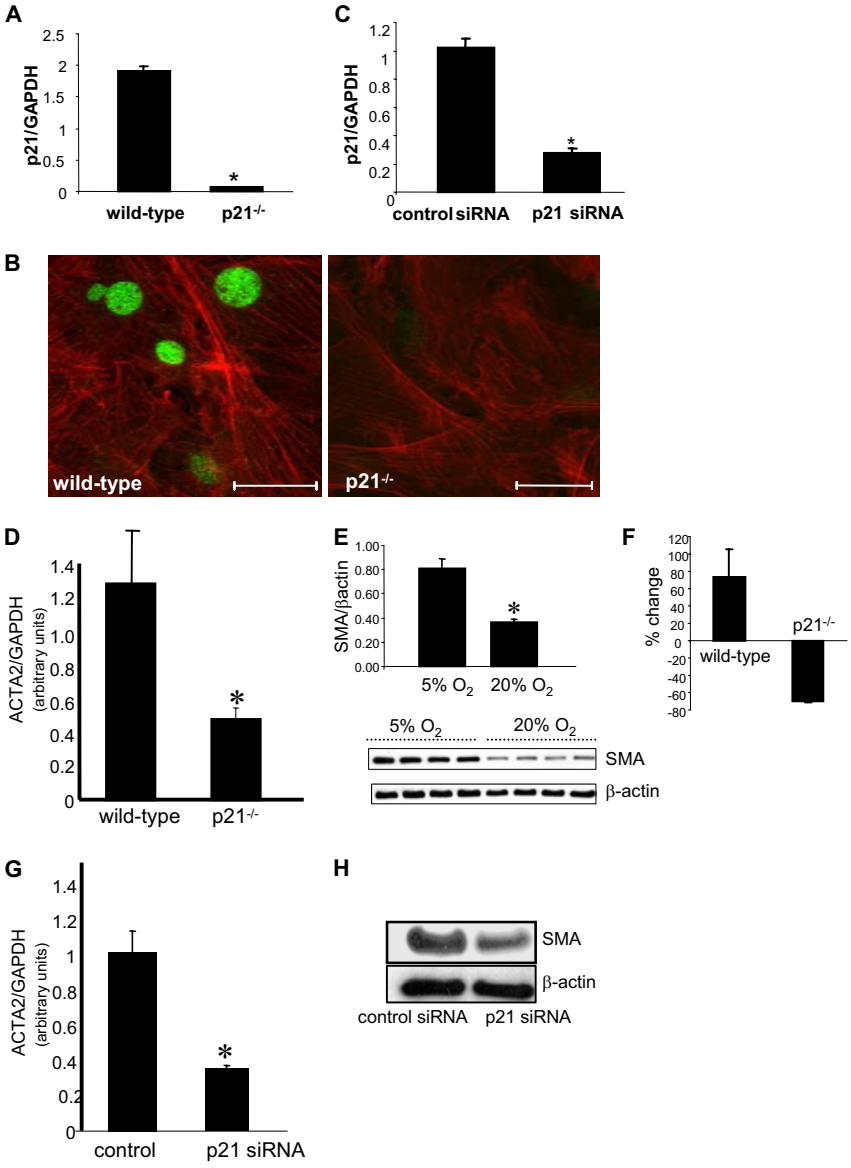

Figure 3. p21 deficiency inhibits oxygen-induced Acta2 mRNA and SMA protein expression in CFs. After isolation, CFs were cultured at 5% O_2 for 5 d. Next, cells were transferred to 5 or 20% O_2 for 5 d. (A) p21 mRNA levels measured using real-time PCR. To eliminate oxygen-induced p21 expression in CFs, cells were harvested from $p21^{-/-}$-deficient mice or the corresponding wild-type $p21^{+/+}$ mice. (A and B) CFs cultured in 20% O_2 for 5 d. p21 mRNA and protein levels in CFs isolated from $p21^{-/-}$ mice compared wild-type $p21^{+/+}$ mice. (A) mRNA levels were determined using real-time PCR. Data ± SD; n = 4. (B) Immunolocalization of p21 protein. Cells stained with anti-p21 antibody (FITC, green) and phalloidin (actin filaments, red). (C) To down-regulate oxygen-induced p21 expression in CFs, cells were harvested from wild-type mice and subjected to p21 knockdown (p21 siRNA) or not (control siRNA). Data ± SD; n = 4. *$p < 0.01$. (D–H) After isolation, CFs were cultured at 5% O_2 (normoxia) for 5 d. Cells were then transferred to 20% O_2 (hyperoxia) for 5 d. (D) Acta2 mRNA levels in CFs isolated from $p21^{-/-}$ mice compared with corresponding wild-type mice. (E) SMA protein levels in CFs isolated from $p21^{-/-}$ mice compared with corresponding wild-type mice. Quantitation of SMA level (bar graph) was performed using densitometry. Data were normalized to β-actin. Data shown represents mean ± SD; n = 4. *$p < 0.01$; significantly lower in CFs from $p21^{-/-}$ than from corresponding wild-type $p21^{+/+}$ mice. (F) Relative O_2-sensitive change in SMA protein levels in CFs isolated from $p21^{-/-}$ mice compared with data from corresponding wild-type mice. Data shown represents % change compared with their respective controls (CFs at 5% O_2). Data are mean ± SD; n = 4. (G) Acta2 mRNA levels in CFs from wild-type mice either subjected to p21 knockdown (p21 siRNA) or not (control scrambled siRNA). Mean ± SD; n = 4); *$p < 0.05$; significantly lower in p21 knockdown cells compared with cells treated with control scrambled siRNA. (H) SMA protein in cells from G.

nificance of p21 in the heart. Cellular differentiation is typically associated with growth-arrest. Therefore, we sought to test whether p21 is implicated in hyperoxia-induced differentiation of CFs to myofibroblasts. To test the significance of p21 in hyperoxia-induced differentiation of CFs to myofibroblasts, it was necessary that we have access to approaches that would reliably down-regulate p21 levels in CFs. To that end, we adopted two strategies. First, we studied CFs isolated from the ventricle of adult $p21^{-/-}$ mice. CFs from these mice and their corresponding wild-type littermates showed striking differences in p21 mRNA (Figure 3A) and protein (Figure 3B) levels. When grown under 20% O_2 hyperoxic conditions p21 in CFs was densely localized in the nucleus. Because knock-out models may suffer from confounding factors such as genomic changes to compensate for the loss of p21, we chose to employ a p21 knockdown model. The knockdown approach utilized in this study resulted in substantial lowering of p21 expression even in CFs cultured in 20% O_2 ambience (Figure 3C). Compared with wild-type mice, Acta2 mRNA level in CFs grown under hyperoxic conditions was significantly lower in CFs from $p21^{-/-}$ mice (Figure 3D). In contrast to the observation in CFs from wild-type mice (Figure 1B), exposure of CFs from $p21^{-/-}$ mice to 20% O_2 lowered the expression of SMA (Figure 3, E and F). These findings indicate a key role of p21 in mediating hyperoxia-induced differentiation of CFs to myofibroblasts. Further support for this contention was obtained from the study of CFs from wild-type mice subjected to p21 knockdown. Compared with CFs grown in 20% O_2 and treated with scrambled siRNA, CFs with p21 knockdown contained lower levels of both Acta2 mRNA as well as SMA expression (Figure 3, G and H).

To characterize the significance of p21 expression on the differentiation of CFs to myofibroblasts, an adenoviral approach to overexpress p21 in CFs cultured at 5% O_2 was adopted. The adenoviral gene transfer approach sharply increased both p21 mRNA (Figure 4A) as well as protein expression (Figure 4B) in CFs. Overexpressed p21 was localized in the nucleus (Figure 4C) as noted for CFs challenged with hyperoxia (Figure 3B). Differentiation of CFs is preceded by growth arrest. We sought to examine the significance of p21 in regulating the cell cycle of CFs. For CFs

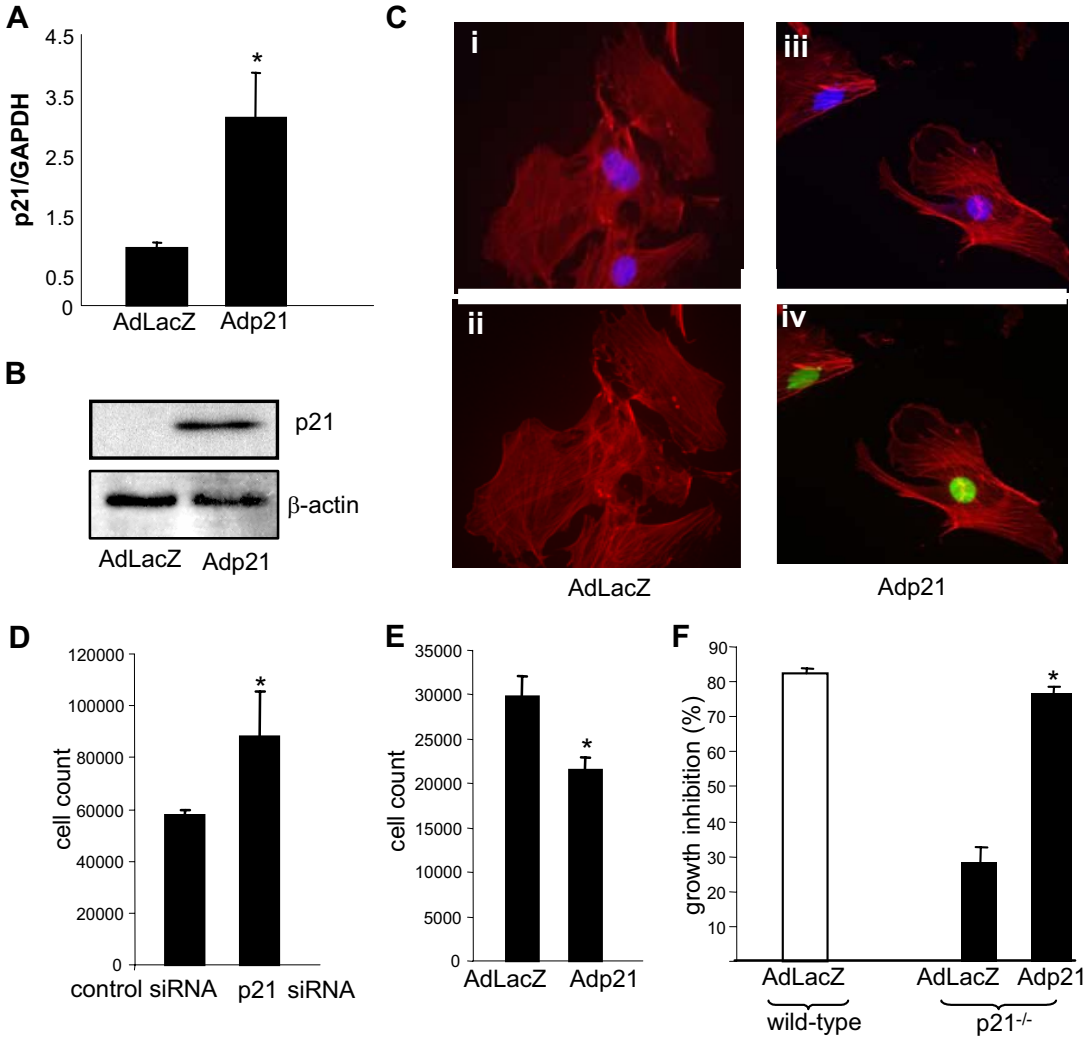

Figure 4. p21 levels in CFs regulate oxygen-induced growth arrest. After isolation, CFs were cultured at 5% O_2 for 5 d followed by splitting and infection with AdLacZ or Adp21 viral vectors for next 24 h. Cells were maintained in 5% O_2 for 5 d. (A) p21 mRNA levels. Mean ± SD, n = 4. *p < 0.01 compared with AdLacZ-infected control cells. (B) Western blot showing effective overexpression of p21 protein in CFs infected with Adp21 virus. (C) Immunofluorescence staining demonstrating overexpression of p21 protein after infection of cells. Cells were stained with anti-p21 antibody (green, FITC), phalloidin (red, actin filaments) and DAPI (blue nucleus). Top panels, (i and iii) DAPI and phalloidin staining; bottom panels, (ii and iv) p21 and phalloidin staining. (D–F) After isolation, CFs were cultured at 5% O_2 for 5 d followed by transfection or infection with p21 siRNA or Adp21 for the next 24 h to down- or up-regulate endogenous p21 levels. (D) CF count in response to p21 knockdown. Cells were cultured at 20% O_2 for 5 d after seeding. (E) CF count in response to p21 overexpression. Cells were cultured at 5% O_2 for 5 d after seeding. Mean ± SD; n = 4. *p < 0.05; significantly different compared with control (control siRNA in D; AdLacZ in E) cells. (F) Count of CFs isolated from $p21^{-/-}$ (■) mice or corresponding wild-type (□) mice. Cells were cultured at 20% O_2 for 5 d followed by infection. CFs from $p21^{-/-}$ were made $p21^{+}$ by infecting the cells with Adp21 viral vector. Data shown represents % inhibition of oxygen-induced cell growth compared with the respective controls (CFs grown at 5% O_2). Mean ± SD; n = 4. *p < 0.01 compared with AdLacZ-infected cells from $p21^{-/-}$ mice. Delivery of p21 to CFs from $p21^{-/-}$ mice restored oxygen-induced growth arrest.

grown in a 20% hyperoxic environment, cell growth was up-regulated in response to p21 knockdown (Figure 4D), indicating an important role of p21 in hyperoxia-induced growth arrest. For CFs grown in 5% normoxic environment, cell growth was significantly inhibited by overexpression of p21 (Figure 4E). Furthermore, lack of sensitivity to hyperoxia-induced growth arrest in p21-deficient CFs could be fully restored by the insertion of p21 (Figure 4F). In this context it is important to note that although hyperoxia induces 80% growth inhibition, ectopic p21 or loss of p21 affects growth inhibition by 25–30%. Although part of this apparent disparity may be explained by the limited (40 ± 10%, not shown) infection efficiency, it is plausible that factors other than p21 may contribute to hyperoxia-induced growth inhibition of cardiac fibroblasts. In light of our previous observation that CFs from p21-deficient mice are insensitive to hyperoxia-induced growth arrest (Roy *et al.*, 2003a), results of the current study led to the conclusion that p21 is central to hyperoxia-induced growth arrest, which precedes differentiation of CFs to myofibroblasts.

To further characterize the significance of p21 on the differentiation to CFs to myofibroblasts, expression of Acta2 and its corresponding protein SMA was studied in CFs. Strikingly, in cells maintained at 5% O_2, overexpression of p21 alone resulted in a marked induction of Acta2 (Figure 5A) as well as SMA (Figure 5B) expression. p21-overexpress-

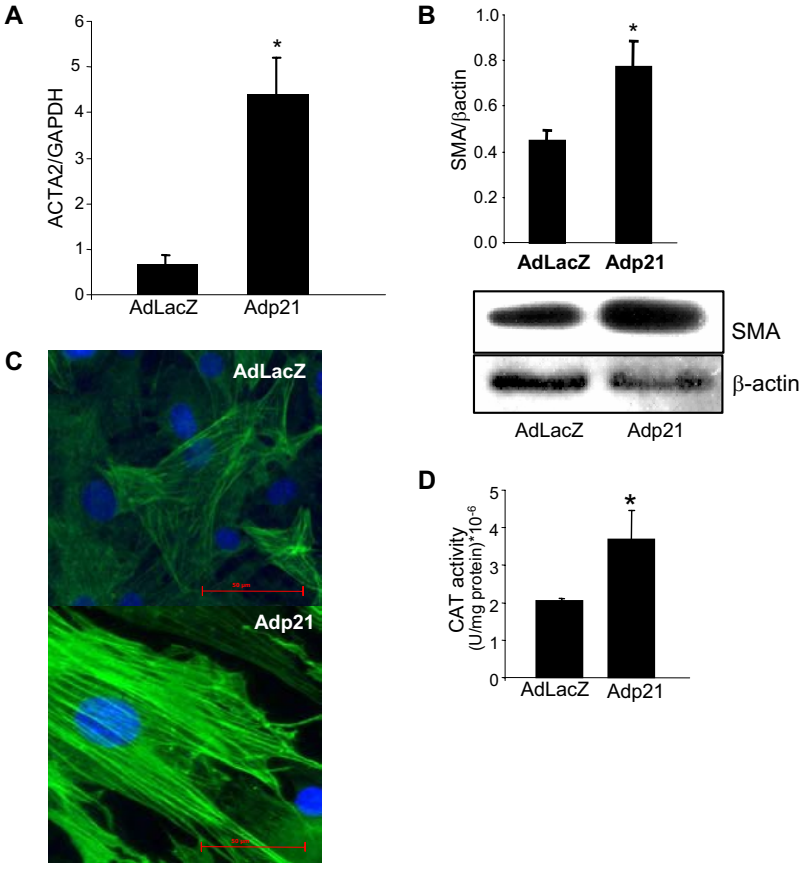

Figure 5. p21 overexpression is sufficient to drive Acta2 mRNA and SMA protein expression in CFs grown under normoxic conditions. Cells were cultured at 5% O_2 (normoxia) and infected as described in Figure 4. (A) Acta2 mRNA levels; mean ± SD, n = 4. *p < 0.01 compared with AdLacZ-infected control cells. (B) SMA expression in CFs; mean ± SD, n = 3. *p < 0.01 compared with AdLacZ-infected control cells. (C) CFs were stained with anti-SMA antibody (FITC, green) and DAPI (blue nucleus). Prominent stress fibers in Adp21 infected cells are characteristic of myofibroblasts. Scale bar, 50 μm. (D) Overexpression of p21 induces SMA promoter-reporter activity. After isolation, CFs were cultured at 5% O_2 for 5 d followed by splitting and infection with AdLacZ or Adp21 for next 24 h. Next, cells were transfected with pVSMP-CAT reporter plasmid and cultured for 5 d at 5% O_2. The CAT activity was determined from cell lysates as an indicator of SMA promoter activity. Result of reporter activity was normalized for the amount of the protein in cell lysates; mean ± SD; n = 4. *p < 0.05; significantly higher compared with cells infected with AdLacZ (control).

ing cells acquired stress fibers and were phenotypically akin to myofibroblasts (Figure 5C). Using a SMA promoter-reporter construct, it was evident that overexpression of p21 alone induces the transcription for SMA (Figure 5D). Although our conclusions are based on differences that are all statistically significant, it is important to recognize that given the limitations in infection efficiency, the differences shown underestimate the true effect.

To address whether adenoviral p21 induction causes growth arrest precedent to differentiation or whether p21 independently induces both processes, time-dependent fluorescence-activated cell sorting analysis of cell cycle and SMA expression was performed. The results show that in response to p21 overexpression, cell cycle arrest and SMA expression are concurrent (Figure 6A). In both cases, significant differences were noted 48 h after p21 infection, suggesting an association between the two processes. Transforming growth factor β1 (TGFβ1) is directly implicated both in cell cycle arrest as well as in triggering differentiation of cardiac fibroblasts (Roy *et al.*, 2003a). To examine whether

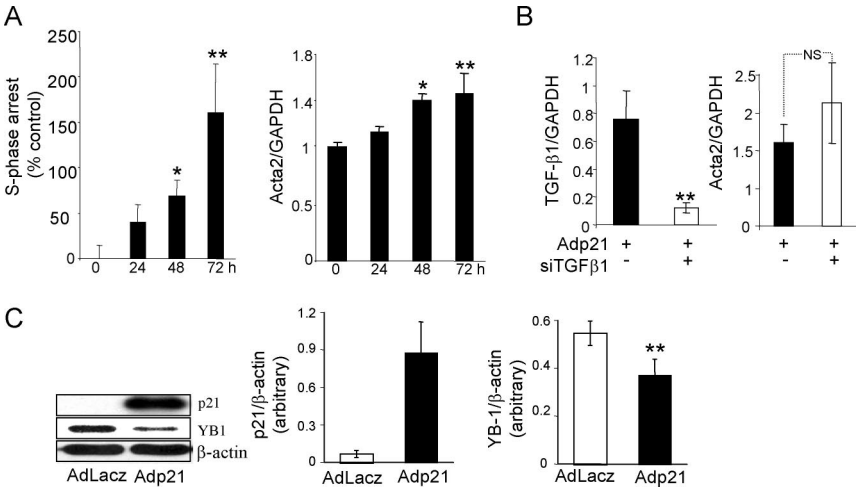

Figure 6. Mechanisms of p21-mediated regulation of Acta2 expression in primary adult cardiac fibroblasts. Cells were cultured at 5% O_2 (normoxia) and infected with Adp21 or AdLacZ as described in Figure 4. (A) Cell cycle analysis (left panel) and Acta2 mRNA expression assay (right panel) were performed as a function of time after Adp21 infection. Cell cycle analysis revealed S-phase arrest in Adp21-infected cells; mean ± SD; n = 3. *p < 0.05; **p < 0.001; significantly higher compared with cells infected with Adp21 at 0 h. (B) p21-overexpressed cells were transfected with TGFβ1 siRNA to knockdown TGFβ1 transcript. CFs transfected with TGFβ1 siRNA resulted in potent down-regulation in TGFβ1 mRNA expression (left panel) ¤ whereas the Acta2 mRNA levels (right panel) under these conditions remained unchanged; mean ± SD; n = 3. **p < 0.001; significantly lower compared with cells transfected with control siRNA; NS, not significantly different. (C) YB-1 protein levels in CFs were measured using Western blot. The blot and quantitative data (bar graphs) are shown; mean ± SD; n = 3. *p < 0.05; significantly higher compared with cells infected with AdLacZ (control).

TGFβ1 is implicated in p21-dependent differentiation of CFs, p21-infected cells were transfected with siRNA against TGFβ1. TGFβ1 knockdown did not lower p21-dependent expression of Acta2, indicating that p21-induced Acta2 expression is independent of TGFβ1 (Figure 6B). Although there is no known p21 binding site in the Acta2 regulatory sequences represented in the CAT reporter construct, the Acta2 regulatory sequence has binding sites for p53 and YB-1. Our group has previously demonstrated that the cold-shock domain protein YB-1 potently represses α-SMA gene transcription in fibroblasts. YB-1 also exhibits additional RNA-binding properties that regulate the translational efficiency of α-SMA mRNA (Kelm *et al.*, 1999; Zhang *et al.*, 2005). Our observation that p21 overexpression significantly down-regulates YB-1 protein expression (Figure 6C) supports the hypothesis that p21 decreases YB-1 levels in cells, thereby withdrawing repressory control of YB-1 on the transcription as well as translation of α-SMA.

The observation that p21 is centrally important to commit the differentiation of CFs to myofibroblasts is a novel finding of outstanding significance. Thus, we sought to examine the relevance of our in vitro findings to myocardial infarction in vivo. Compared with myocytes, CFs are relatively more resistant to oxidant insult (Zhang *et al.*, 2001). As such, portions of the infarct tissue from which myocytes have been lost to death retain CFs. Recently we have developed a laser capture–based technique to selectively study gene and protein expression in specific regions of the infarcted heart (Kuhn *et al.*, 2006, 2007; Roy *et al.*, 2006a). The approach enabled us to collect tissue elements from the myocyte$^-$/CF$^+$ infarct region and compare it with results from myocyte$^+$/CF$^+$ tissue elements collected <0.5 mm away from the infarct region (Figure 7A). Ischemia-reperfusion resulted in marked p21 induction in the myocyte$^-$/CF$^+$ infarct region (Figure 7B). Consistent with our hypothesis that the surviving CFs at the infarct site undergo phenotypic switch to form myofibroblasts, Acta2 mRNA (Figure 7C) as well as SMA protein (Figure 7, D and E) expression were markedly up-regulated in the CF-rich infarct region. Of note, ischemia-reperfusion induced up-regulation of Acta2 mRNA in the infarct region was completely abrogated in p21-deficient mice (Figure 7F). This observation establishes that p21 is a central regulator of reperfusion-induced phenotypic switch of CFs to myofibroblasts in the infarct region.

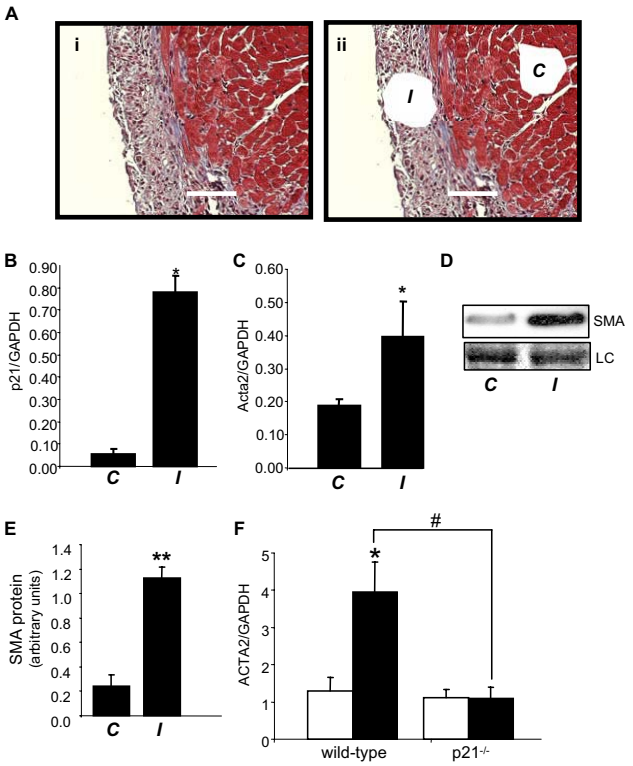

Figure 7. Induction of Acta2 mRNA and SMA protein in CF$^+$myocyte$^-$ infarct region of the ischemia-reperfused murine heart. C57BL/6 mice were subjected to ischemia (30 min) and reperfusion for 7 d. (A–C) Frozen sections (10 μm) from the affected site of the heart stained with hematoxylin-eosin to histologically define the boundary of the infarct (*I*) and control (*C*, CF$^+$myocyte$^+$ region at the affected site) areas in the same microscopic field. (i) Representative stained frozen section; (ii) the same section as shown in panel i after the tissue elements from *I* and *C* regions have been laser captured. Scale bar, 100 μm. The captured tissue was used for quantification of p21 and Acta2 mRNA, and SMA protein; (B) p21 mRNA. (C) Acta2 mRNA; mean ± SEM; n = 4. *p < 0.05 higher in *I* compared with *C* tissues. (D–F) Control (*C*) and infarct (*I*) tissues were collected, and SMA protein level was quantified. (D) Western blot of SMA. (E) Quantification of Western blot (D) was performed using densitometry. Data were normalized against a loading control detected on Ponceau-stained membrane. LC, loading control. Mean ± SD; n = 3. *p < 0.05; significantly higher in *I* compared with tissue elements captured from the *C* region. (F) Ischemia-reperfusion induced induction of Acta2 mRNA expression in the boundary of the infarct region was completely abrogated in p21$^{-/-}$ mice. p21$^{-/-}$ or matching wild-type mice were subjected to ischemia (30 min) followed by reperfusion for 7 d. *I* (■) and *C* (□) tissue elements were laser captured. Acta2 and GAPDH mRNA levels were quantified using real-time PCR; mean ± SEM; n = 4. *p < 0.05; significantly higher compared with control (*C*) tissue. #p < 0.05; significantly lower in p21$^{-/-}$ compared with results from p21$^{+/+}$ wild-type animals.

DISCUSSION

In excess of 90% of the myocardium's interstitial cells are fibroblasts (Eghbali *et al.*, 1988), which actively cross-talk with myocytes to determine the quantity and quality of extracellular matrix. Compared with myocytes, CFs are relatively more resistant to oxidant insult (Zhang *et al.*, 2001). Under certain pathological conditions such as aortic regurgitation, CFs produce abnormal proportions of noncollagen extracellular matrix, specifically fibronectin, with relatively little change in collagen synthesis (Borer *et al.*, 2002). A characteristic feature of CFs is their ability to differentiate forming myofibroblasts. Phenotypic switching of CFs to myofibroblast is controlled by a variety of growth factors, cytokines, and mechanical stimuli (Powell *et al.*, 1999; Serini and Gabbiani, 1999; Tomasek *et al.*, 2002). Activation of CFs and cardiac ECM remodeling is necessary after myocardial injury. However, limiting prolonged fibroblast activation and subsequent detrimental extracellular matrix production is a potential approach to preserving left ventricular function. Thus, understanding of the molecular mechanisms regulating differentiation of CFs to myofibroblast may provide a means to inhibit maladaptive tissue remodeling in response to profibrotic stimuli and facilitate the endogenous healing response to injury (Tomasek *et al.*, 2002).

The current study provides novel mechanistic insight into how relative hyperoxic shock, as noted during ischemia-reoxygenation of the heart, may serve as a trigger for the phenotypic switch of CFs to myofibroblasts. Recently, the NADPH oxidase family member Nox4 has been implicated in the differentiation of CFs to myofibroblasts. The reactive oxygen species superoxide mediated the TGFβ1-induced CF

differentiation process (Cucoranu *et al.*, 2005). The mechanism described in the current study is distinct from that report because relative hyperoxia-induced transformation of CFs to myofibroblasts has been noted in CFs derived from NADPH oxidase–deficient mice (Roy *et al.*, 2003b). Furthermore, differentiation of CFs to myofibroblasts in response to hyperoxic challenge was not sensitive to antioxidant strategies such as catalase overexpression or treatment of cells with *N*-acetylcysteine (Roy *et al.*, 2003b). The present work presents first evidence identifying p21 as being singularly sufficient to trigger a phenotypic switch of CFs to myofibroblasts. This finding is consistent with the notion proposed by Nabel (2002) that many of the signaling pathways that control cellular decisions related to tissue remodeling are regulated by nuclear interactions of cell cycle proteins. She rationalized that molecules targeting cyclin-dependent kinases (CDK) or CDK inhibitors (CKI) represent a new class of therapeutic agents that influence tissue remodeling in several organ systems. p21 is a CKI, and the results reported herein are in agreement with the proposal put forth by Nabel.

The cyclin-dependent kinase inhibitor p21 is a major player in cell cycle control. Although induction of p21 predominantly leads to cell cycle arrest, repression of p21 is known to have a variety of outcomes, depending on the context. p21-activated kinases regulate cytoskeletal remodeling (Kumar *et al.*, 2006). Functions of p21, beyond its role as a cell cycle brake, have been hypothesized (Coqueret, 2003). Results of this study identify p21 as a key regulator of the differentiation of CFs to myofibroblasts. TGFβ is a well-known natural inducer of growth inhibition and differentiation in CFs (Frangogiannis *et al.*, 2000; Bujak and Frangogiannis, 2007). Growth arrest caused by TGFβ is mediated through interactions of CDK and CKI. TGFβ induces increased levels of p21 (Li *et al.*, 1995; Reynisdottir *et al.*, 1995; Bachman *et al.*, 2004; Wada *et al.*, 2005). In vascular smooth muscle cells, specific inhibition of p21 protein markedly reduced the production and secretion of the matrix proteins fibronectin and laminin both in the presence and absence of TGFβ stimulation (Weiss and Randour, 2002). Thus, consistent with the findings of the current study noting a lack of TGFβ1 involvement in p21-induced Acta2 expression, the literature suggest that TGFβ is upstream of p21 in the signaling cascade leading to cell cycle arrest and differentiation.

Myofibroblast differentiation is a complex process, regulated by at least a cytokine (TGFβ1) and an extracellular matrix component (the ED-A splice variant of cellular fibronectin), as well as the presence of mechanical tension (Desmouliere *et al.*, 2005). Mechanical tension controls granulation tissue contractile activity and myofibroblast differentiation (Hinz *et al.*, 2001). The myocardium responds to chronic pressure or volume overload by activation and proliferation of CFs and their differentiation into myofibroblasts. Mechanical stretch has been shown to induce p21 in CFs (Liao *et al.*, 2004). Although it is thought that such induction may be responsible for stretch-induced G2/M arrest of CFs, the functional significance of p21 in CF differentiation was not tested. Results of the current study demonstrate that down-regulation of YB-1, a potent repressor of SMA gene transcription, represents a plausible mechanism by which p21 induces SMA expression. TP53, a key protein involved in the transcription of p21 directly interacts with YB-1 and regulates gene expression (Okamoto *et al.*, 2000). Findings reported in this work raise the possibility that mechanical stretch and hyperoxic challenge both cause differentiation of CFs by a common downstream mechanism, e.g., induction of p21. As a CKI, p21 is functional when it is localized in the nucleus. Interestingly, pancreatic myofibroblasts have been observed to contain elevated levels of p21. Withdrawal of p21 from the nucleus to the cytoplasm correlated with dedifferentiation of pancreatic myofibroblast to fibroblast (Manapov *et al.*, 2005). Although these results are not relevant to cells of the heart, they represent valuable reference material, suggesting that the observation of this study identifying p21 as a key determinant of CF differentiation may have broader significance explaining the molecular mechanisms underlying fibrosis across organ types.

The growth-suppressive activities of hyperoxia are known to be mediated, in part, through induction of p21. Using SV40-transformed type II epithelial cells exposed to hyperoxia, Corroyer *et al.* (1996) were the first to show that hyperoxia induces p21. Subsequent studies in a variety of nontransformed cell lines confirmed that hyperoxia inhibited cell proliferation through induction of p21. Hyperoxia also increased p21 mRNA and protein in terminal bronchiole epithelium and alveolar endothelial and type I and II epithelial cells of adult and newborn mice (Staversky *et al.*, 2002). We recently showed that hyperoxia inhibited cell proliferation of CFs from adult wild-type, but not from p21-deficient mice. Consistent results have been noted in the lung (O'Reilly *et al.*, 2001). This study presents first evidence that beyond causing growth arrest, p21 may act as a trigger for the differentiation of CFs. Thus, p21 may be viewed as a major mediator of ventricular remodeling of the reoxygenated heart.

One of the key determinants of the response of CFs in the clinical context of myocardial damage is its transformation from a quiescent cell primarily responsible for ECM homeostasis, to an activated or differentiated cell that plays a central role in wound healing or fibrosis, depending on the circumstances. The current study identifies a novel opportunity to differentiate CFs by modulating p21 expression. This finding has direct implications in wound healing and in limiting fibrosis after myocardial infarction. The contribution of cardiac fibrosis as an independent risk factor in the outcome of heart failure has been evaluated (Brown *et al.*, 2005). At present, the candidate drug therapies that derive benefit from actions on CFs include inhibitors of angiotensin-aldosterone systems, endothelin receptor antagonists, statins, anticytokine therapies, matrix metalloproteinase inhibitors, and novel antifibrotic/anti-inflammatory agents (Brown *et al.*, 2005). That low oxygen ambience serves as a cue to trigger angiogenesis is a well-accepted notion. Studies related to perceived hyperoxia establish that the sensing of O_2 environment is not limited to hypoxia. It demonstrates that in addition to being a trigger for injury as is widely recognized, reoxygenation insult triggers remodeling response via a p21-dependent mechanism. Understanding the underlying mechanisms of this healing response should prove to be instrumental in developing productive therapeutic approaches targeting the CKI pathway.

ACKNOWLEDGMENTS

This work was supported by National Institutes of Health awards RO1 HL073087, GM 077185 and GM 069589 to C.K.S.

REFERENCES

Bachman, K. E., Blair, B. G., Brenner, K., Bardelli, A., Arena, S., Zhou, S., Hicks, J., De Marzo, A. M., Argani, P., and Park, B. H. (2004). p21(WAF1/CIP1) mediates the growth response to TGF-beta in human epithelial cells. Cancer Biol. Ther. *3*, 221–225.

Borer, J. S., Truter, S., Herrold, E. M., Falcone, D. J., Pena, M., Carter, J. N., Dumlao, T. F., Lee, J. A., and Supino, P. G. (2002). Myocardial fibrosis in chronic aortic regurgitation: molecular and cellular responses to volume overload. Circulation *105*, 1837–1842.

Brilla, C. G. (2000). Renin-angiotensin system mediated mechanisms: cardioreparation and cardioprotection. Heart *84*(Suppl 1), i18–i19, discussion, i50.

Brown, R. D., Ambler, S. K., Mitchell, M. D., and Long, C. S. (2005). The cardiac fibroblast: therapeutic target in myocardial remodeling and failure. Annu. Rev. Pharmacol. Toxicol. *45*, 657–687.

Bujak, M., and Frangogiannis, N. G. (2007). The role of TGF-beta signaling in myocardial infarction and cardiac remodeling. Cardiovasc. Res. *74*, 184–195.

Burlew, B. S., and Weber, K. T. (2002). Cardiac fibrosis as a cause of diastolic dysfunction. Herz *27*, 92–98.

Capasso, J. M., Palackal, T., Olivetti, G., and Anversa, P. (1990). Severe myocardial dysfunction induced by ventricular remodeling in aging rat hearts. Am. J. Physiol. *259*, H1086–H1096.

Coqueret, O. (2003). New roles for p21 and p27 cell-cycle inhibitors: a function for each cell compartment? Trends Cell Biol. *13*, 65–70.

Corroyer, S., Maitre, B., Cazals, V., and Clement, A. (1996). Altered regulation of G1 cyclins in oxidant-induced growth arrest of lung alveolar epithelial cells. Accumulation of inactive cyclin E-DCK2 complexes. J. Biol. Chem. *271*, 25117–25125.

Cucoranu, I., Clempus, R., Dikalova, A., Phelan, P. J., Ariyan, S., Dikalov, S., and Sorescu, D. (2005). NAD(P)H oxidase 4 mediates transforming growth factor-beta1-induced differentiation of cardiac fibroblasts into myofibroblasts. Circ. Res. *97*, 900–907.

Desmouliere, A., Chaponnier, C., and Gabbiani, G. (2005). Tissue repair, contraction, and the myofibroblast. Wound Repair Regen. *13*, 7–12.

Eghbali, M., Czaja, M. J., Zeydel, M., Weiner, F. R., Zern, M. A., Seifter, S., and Blumenfeld, O. O. (1988). Collagen chain mRNAs in isolated heart cells from young and adult rats. J. Mol. Cell. Cardiol. *20*, 267–276.

Foster, D. N., Min, B., Foster, L. K., Stoflet, E. S., Sun, S., Getz, M. J., and Strauch, A. R. (1992). Positive and negative cis-acting regulatory elements mediate expression of the mouse vascular smooth muscle alpha-actin gene. J. Biol. Chem. *267*, 11995–12003.

Frangogiannis, N. G. (2006). The mechanistic basis of infarct healing. Antioxid. Redox Signal. *8*, 1907–1939.

Frangogiannis, N. G., Michael, L. H., and Entman, M. L. (2000). Myofibroblasts in reperfused myocardial infarcts express the embryonic form of smooth muscle myosin heavy chain (SMemb). Cardiovasc Res. *48*, 89–100.

Hinz, B., Mastrangelo, D., Iselin, C. E., Chaponnier, C., and Gabbiani, G. (2001). Mechanical tension controls granulation tissue contractile activity and myofibroblast differentiation. Am. J. Pathol. *159*, 1009–1020.

Kelm, R. J., Jr., Cogan, J. G., Elder, P. K., Strauch, A. R., and Getz, M. J. (1999). Molecular interactions between single-stranded DNA-binding proteins associated with an essential MCAT element in the mouse smooth muscle alpha-actin promoter. J. Biol. Chem. *274*, 14238–14245.

Khanna, S., Roy, S., Maurer, M., Ratan, R. R., and Sen, C. K. (2006). Oxygen-sensitive reset of hypoxia-inducible factor transactivation response: Prolyl hydroxylases tune the biological normoxic set point. Free Radic Biol. Med. *40*, 2147–2154.

Krishan, A. (1975). Rapid flow cytofluorometric analysis of mammalian cell cycle by propidium iodide staining. J. Cell Biol. *66*, 188–193.

Kuhn, D., Roy, S., Radtke, J., Khanna, S., and Sen, C. K. (2007). Laser microdissection and capture of pure cardiomyocytes and fibroblasts from infarcted heart regions: perceived hyperoxia induces P21 in peri-infarct myocytes. Am. J. Physiol. Heart Circ. Physiol. *292*, H1245–H1253.

Kuhn, D. E., Roy, S., Radtke, J., Gupta, S., and Sen, C. K. (2006). Laser microdissection and pressure-catapulting technique to study gene expression in the reoxygenated myocardium. Am. J. Physiol. Heart Circ. Physiol. *290*, H2625–H2632.

Kumar, R., Gururaj, A. E., and Barnes, C. J. (2006). p21-activated kinases in cancer. Nat. Rev. Cancer *6*, 459–471.

Laframboise, W. A., Scalise, D., Stoodley, P., Graner, S., Guthrie, R. D., Magovern, J., and Becich, M. (2007). Cardiac fibroblasts influence cardiomyocyte phenotype in vitro. Am. J. Physiol. Cell Physiol. *292(5)*, C1799–C1808.

Li, C. Y., Suardet, L., and Little, J. B. (1995). Potential role of WAF1/Cip1/p21 as a mediator of TGF-beta cytoinhibitory effect. J. Biol. Chem. *270*, 4971–4974.

Liao, X. D., Wang, X. H., Jin, H. J., Chen, L. Y., and Chen, Q. (2004). Mechanical stretch induces mitochondria-dependent apoptosis in neonatal rat cardiomyocytes and G2/M accumulation in cardiac fibroblasts. Cell Res. *14*, 16–26.

Manapov, F., Muller, P., and Rychly, J. (2005). Translocation of p21(Cip1/WAF1) from the nucleus to the cytoplasm correlates with pancreatic myofibroblast to fibroblast cell conversion. Gut *54*, 814–822.

Min, B. H., Foster, D. N., and Strauch, A. R. (1990). The 5′-flanking region of the mouse vascular smooth muscle alpha-actin gene contains evolutionarily conserved sequence motifs within a functional promoter. J. Biol. Chem. *265*, 16667–16675.

Miragoli, M., Gaudesius, G., and Rohr, S. (2006). Electrotonic modulation of cardiac impulse conduction by myofibroblasts. Circ. Res. *98*, 801–810.

Nabel, E. G. (2002). CDKs and CKIs: molecular targets for tissue remodelling. Nature Rev. Drug Disc. *1*, 587–598.

Naugle, J. E., Olson, E. R., Zhang, X., Mase, S. E., Pilati, C. F., Maron, M. B., Folkesson, H. G., Horne, W. I., Doane, K. J., and Meszaros, J. G. (2006). Type VI collagen induces cardiac myofibroblast differentiation: implications for postinfarction remodeling. Am. J. Physiol. Heart Circ. Physiol. *290*, H323–H330.

O'Reilly, M. A., Staversky, R. J., Watkins, R. H., Reed, C. K., de Mesy Jensen, K. L., Finkelstein, J. N., and Keng, P. C. (2001). The cyclin-dependent kinase inhibitor p21 protects the lung from oxidative stress. Am. J. Respir Cell. Mol. Biol. *24*, 703–710.

Okamoto, T., Izumi, H., Imamura, T., Takano, H., Ise, T., Uchiumi, T., Kuwano, M., and Kohno, K. (2000). Direct interaction of p53 with the Y-box binding protein, YB- 1, a mechanism for regulation of human gene expression. Oncogene *19*, 6194–6202.

Powell, D. W., Mifflin, R. C., Valentich, J. D., Crowe, S. E., Saada, J. I., and West, A. B. (1999). Myofibroblasts. I. Paracrine cells important in health and disease. Am. J. Physiol. *277*, C1–C9.

Reynisdottir, I., Polyak, K., Iavarone, A., and Massague, J. (1995). Kip/Cip and Ink4 Cdk inhibitors cooperate to induce cell cycle arrest in response to TGF-beta. Genes Dev. *9*, 1831–1845.

Roy, S. *et al.* (2003a). Oxygen sensing by primary cardiac fibroblasts: a key role of p21(Waf1/Cip1/Sdi1). Circ. Res. *92*, 264–271.

Roy, S., Khanna, S., Kuhn, D. E., Rink, C., Williams, W. T., Zweier, J. L., and Sen, C. K. (2006a). Transcriptome analysis of the ischemia-reperfused remodeling myocardium: temporal changes in inflammation and extracellular matrix. Physiol. Genomics *25*, 364–374.

Roy, S., Khanna, S., Nallu, K., Hunt, T. K., and Sen, C. K. (2006b). Dermal wound healing is subject to redox control. Mol. Ther. *13*, 211–220.

Roy, S., Khanna, S., Wallace, W. A., Lappalainen, J., Rink, C., Cardounel, A. J., Zweier, J. L., and Sen, C. K. (2003b). Characterization of perceived hyperoxia in isolated primary cardiac fibroblasts and in the reoxygenated heart. J. Biol. Chem. *278*, 47129–47135.

Sen, C. K., Khanna, S., and Roy, S. (2006). Perceived hyperoxia: oxygen-induced remodeling of the reoxygenated heart. Cardiovasc. Res. *71*, 280–288.

Serini, G., and Gabbiani, G. (1999). Mechanisms of myofibroblast activity and phenotypic modulation. Exp. Cell Res. *250*, 273–283.

Siaghy, E. M., Devaux, Y., Sfaksi, N., Carteaux, J. P., Ungureanu-Longrois, D., Zannad, F., Villemot, J. P., Burlet, C., and Mertes, P. M. (2000). Consequences of inspired oxygen fraction manipulation on myocardial oxygen pressure, adenosine and lactate concentrations: a combined myocardial microdialysis and sensitive oxygen electrode study in pigs. J. Mol. Cell. Cardiol. *32*, 493–504.

Staversky, R. J., Watkins, R. H., Wright, T. W., Hernady, E., LoMonaco, M. B., D'Angio, C. T., Williams, J. P., Maniscalco, W. M., and O'Reilly, M. A. (2002). Normal remodeling of the oxygen-injured lung requires the cyclin-dependent kinase inhibitor p21(Cip1/WAF1/Sdi1). Am. J. Pathol. *161*, 1383–1393.

Sun, Y., Zhang, J. Q., Zhang, J., and Lamparter, S. (2000). Cardiac remodeling by fibrous tissue after infarction in rats. J. Lab. Clin. Med. *135*, 316–323.

Swaney, J. S., Roth, D. M., Olson, E. R., Naugle, J. E., Meszaros, J. G., and Insel, P. A. (2005). Inhibition of cardiac myofibroblast formation and collagen synthesis by activation and overexpression of adenylyl cyclase. Proc. Natl. Acad. Sci. USA *102*, 437–442.

Tomasek, J. J., Gabbiani, G., Hinz, B., Chaponnier, C., and Brown, R. A. (2002). Myofibroblasts and mechano-regulation of connective tissue remodelling. Nat. Rev. Mol. Cell Biol. *3*, 349–363.

Wada, T., Pippin, J. W., Terada, Y., and Shankland, S. J. (2005). The cyclin-dependent kinase inhibitor p21 is required for TGF-beta1-induced podocyte apoptosis. Kidney Int. *68*, 1618–1629.

Weber, K. T., and Brilla, C. G. (1991). Pathological hypertrophy and cardiac interstitium. Fibrosis and renin-angiotensin-aldosterone system. Circulation *83*, 1849–1865.

Weiss, R. H., and Randour, C. J. (2002). Attenuation of matrix protein secretion by antisense oligodeoxynucleotides to the cyclin kinase inhibitor p21(Waf1/Cip1). Atherosclerosis *161*, 105–112.

Zhang, A., Liu, X., Cogan, J. G., Fuerst, M. D., Polikandriotis, J. A., Kelm, R. J., Jr., and Strauch, A. R. (2005). YB-1 coordinates vascular smooth muscle alpha-actin gene activation by transforming growth factor beta1 and thrombin during differentiation of human pulmonary myofibroblasts. Mol. Biol. Cell *16*, 4931–4940.

Zhang, X., Azhar, G., Nagano, K., and Wei, J. Y. (2001). Differential vulnerability to oxidative stress in rat cardiac myocytes versus fibroblasts. J. Am. Coll. Cardiol. *38*, 2055–2062.